Density-induced geometric frustration of ultra-cold bosons in optical lattices

2016 New J. Phys. 18 045016

(http://iopscience.iop.org/1367-2630/18/4/045016)

New Journal of Physics
The open access journal at the forefront of physics

Deutsche Physikalische Gesellschaft DPG
IOP Institute of Physics

Published in partnership with: Deutsche Physikalische Gesellschaft and the Institute of Physics

PAPER

OPEN ACCESS

RECEIVED
3 December 2015

REVISED
23 March 2016

ACCEPTED FOR PUBLICATION
29 March 2016

PUBLISHED
19 April 2016

Density-induced geometric frustration of ultra-cold bosons in optical lattices

T Mishra[1,2], **S Greschner**[1] **and L Santos**[1]

[1] Institut für Theoretische Physik, Leibniz Universität Hannover, D-30167 Hannover, Germany
[2] Indian Institute of Technology Guwahati, Guwahati, 781039, India

E-mail: mishratapan@iitg.ernet.in

Keywords: synthetic magnetism, kinetic frustration, ultracold gases

Abstract

A density-dependent gauge field may induce density-induced geometric frustration, leading to a non-trivial interplay between density modulation and frustration, which we illustrate for the particular case of ultra-cold bosons in zig-zag optical lattices with a density-dependent hopping amplitude. We show that the density-induced frustration leads to a rich landscape of quantum phases, including Mott insulator, bond-order insulator, two-component superfluids, chiral superfluids, and partially paired superfluids. We show as well that the density-dependent hopping results in an effective repulsive or attractive interaction, and that for the latter case the vacuum may be destabilized leading to a strong compressibility. Finally, we discuss the characteristic momentum distribution of the predicted phases, which can be used to detect the phases in time-of-flight measurements.

1. Introduction

Geometric frustration, especially in low-dimensional systems, results in the stabilization of unusual quantum phases [1]. Ultra-cold atoms in optical lattices constitute an excellent environment for the study of the effects of geometric frustration in quantum many-body systems, due to the exquisite experimental control available over the lattice geometry, including triangular [2] and kagome [3] lattices, and even lattices with variable geometry [4, 5]. Geometric frustration may result as well from the careful manipulation of the hopping rates. Lattice shaking has been already employed to change selectively the sign of the hopping rate along some directions in the lattice [6], or even to obtain complex hopping rates [2]. Complex hopping rates have been realized as well by means of Raman-assisted hopping, a technique that has recently allowed for the successful realization of synthetic magnetic fields [7–11].

Up to now, the created synthetic gauge fields, and in general the hopping rates in the lattice, are not affected by the atoms, i.e. the created gauge fields and lattice geometries are static. Recently, it has been proposed that laser-assisted hopping may result in the realization of density-dependent gauge fields [12–15] for which the hopping rates (in particular their phase) is dynamically modified depending on the local lattice occupation number. In one-dimensional lattices density-dependent gauge fields result in the anyon-Hubbard model [12, 13], which is characterized by gauge-driven Mott-insulator (MI) to superfluid (SF) transitions, Mott phases at negative on-site interactions, and by the appearance of novel phases (in particular the so-called partially paired superfluid (PP) [13]). In higher-dimensions, laser-assisted hopping may induce under proper conditions density-dependent magnetism, which results in a non-trivial interplay between density modulation and chirality [14].

These recently proposed techniques for creating density-dependent hopping rates not only allow for the creation of density-dependent magnetism; more generally they open interesting possibilities for the study of lattice models with an occupation-dependent geometric frustration. In this paper, we will illustrate the non-trivial interplay between lattice occupation and frustration in these models for the particular case of ultra-cold atoms in zig-zag lattices (see figure 1). Zig-zag lattices are equivalent to one-dimensional lattices with nearest- and next-nearest-neighbor hoppings, and have been extensively investigated in the presence of frustration

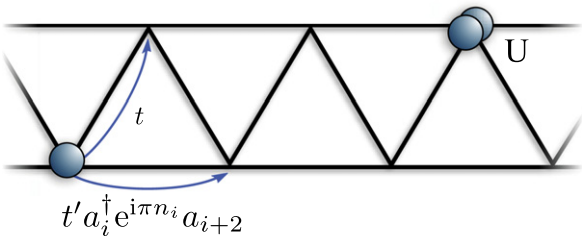

Figure 1. Schematic diagram of the zig-zag lattice with density-dependent next-nearest neighbor hopping considered in this paper.

[16–20, 22–26]. They may be easily realized with ultra-cold atoms in optical lattices by superimposing incoherently a one-dimensional lattice and a triangular lattice, as shown in [23]. We show below, that the occupation-dependent frustration results in a very rich landscape of insulator and superfluid phases, including chiral superfluids (CSF), two-component superfluids (2SF), MI phases with string order, bond-order insulators (BO), and the PP phase.

2. Model and method

We consider a system of ultra-cold bosons in a zig-zag optical lattice with density dependent frustration as depicted in figure 1. The hopping rate along the rungs (legs) is denoted as t (t'). The coupling constant U represents the two-body on-site repulsion between the atoms. Density-dependent frustration is realized by associating a density dependent Peierls phase to t' (for a discussion on how these occupation dependent phases may be created by means of Raman-assisted hopping we refer to the detail discussions in [13, 14]). The system is described by the Bose–Hubbard Hamiltonian:

$$H = -t\sum_i (a_i^\dagger a_{i+1} + \text{H.c.}) - t'\sum_i (a_i^\dagger e^{i\pi n_i} a_{i+2} + \text{H.c.}) + \frac{U}{2}\sum_i n_i(n_i - 1), \tag{1}$$

where $a_i^\dagger$, a_i , and $n_i = a_i^\dagger a_i$ are creation, annihilation, and number operators for bosons at site i. As discussed in [13, 14], the scheme employed to create the density-dependent Peierls phase also results in an on-site two-body hardcore constraint (2BHCC), $(a_i^\dagger)^3 = 0$, i.e. a maximum of two bosons may occupy a given site. For simplicity, we set $t = 1$ as the energy scale in the following.

Recent studies on ultra-cold bosons with 2BHCC and an occupation-independent tunneling in a fully-frustrated zig-zag lattice ($t' < 0$ and $t > 0$) have shown that the system undergoes a transition from a SF to a gapped Haldane-insulator (HI) phase and then to a CSF phase as a function of frustration (i.e. as a function of $|t'|/t$) at unit filling and $U = 0$ [23]. For $U < 0$ the system exhibits transitions to other phases such as pair-superfluid (PSF) and density wave (DW). On the other hand a system of hardcore bosons ($U = \infty$) in a fully frustrated zig-zag lattice resembles an isotropic $J_1 - J_2$ model with some quantitative differences. The phase diagram of this system is dominated by the BO phase at intermediate values of $|t'|$, whereas for large t' the system CSF phase [24–26].

In this paper we are especially interested in the effects that the density-dependent phase of the next-nearest neighbor hopping in Model (1) (and hence the corresponding occupation-dependent geometric frustration) has on the ground-state properties of the system. We will hence restrict for simplicity to the case $U = 0$ (note however, that the system remains effectively interacting due to the 2BHCC, and the occupation-dependent hopping itself), and obtain the ground-state phase diagram as a function of the frustrated hopping and the lattice filling using the density matrix renormalization group (DMRG) method [27, 28] for up to 120 lattice sites and 300 density matrix eigenstates.

3. Single particle dispersion

Important aspects of the physics of the zig-zag lattice may be understood from its single particle dispersion, valid for the limit of low lattice filling, $\rho \to 0$

$$\epsilon(k) = -2t\cos k - 2t'\cos 2k. \tag{2}$$

For $t' < 0$ the model is frustrated, and for $|t'|/t > 1/4$ the dispersion relation presents two degenerate minima at distinct momenta $k = \pm Q \equiv \pm\arccos(t/4|t'|)$. Due to this degeneracy the effect of interactions becomes crucial for selecting a particular ground-state. Typically the two phases are found in the density-independent

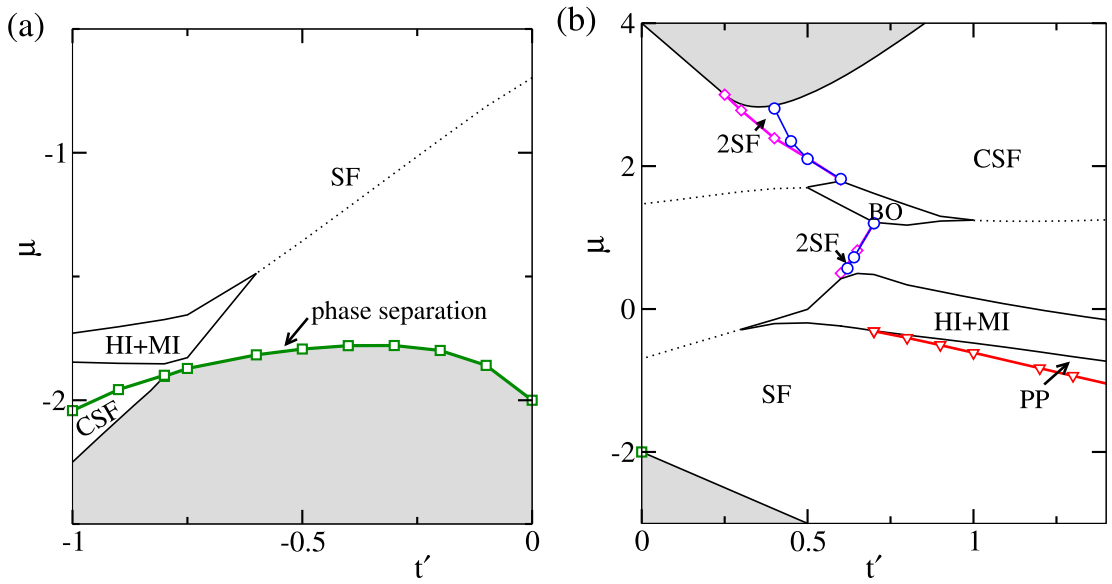

Figure 2. Ground-state phase diagram of Model (1) for $t' < 0$ (a) and $t' > 0$ (b). The gapped MI+HI and BO phases are bounded by the black solid curves. For $t' > 0$ the PP phase is below the MI+HI phase, and the SF–PP transition is marked by red triangles. The 2SF phase is bounded between the magenta diamonds and blue circles. The CSF phase (at the right of the blue circles) covers a broad range of the phase diagram. For $t' < 0$, the abrupt density jump (phase separation) is marked by green squares. In both figures, the gray regions represent the empty ($\rho = 0$) and full ($\rho = 2$) states.

model [29]: a two-component 2SF phase, in which the particles occupy both minima equally; a one-component CSF phase, with all particles quasi-condensing in one of the two minima, which is spontaneously selected. Hence the CSF phase in the thermodynamic limit is twofold degenerate and exhibits a non-vanishing local boson current or chirality

$$\chi_i = \frac{\mathrm{i}}{2}(a_i^\dagger a_{i+1} - \mathrm{H.c.}). \tag{3}$$

In a finite system this locally defined chirality is always zero. However, the CSF phase is clearly characterized by the long-range ordered current-current correlations (chiral order parameter)

$$\kappa = \lim_{|i-j|\gg 1} \langle \chi_i \chi_j \rangle. \tag{4}$$

The 2SF phase does not exhibit a finite chirality. We will discuss a more quantitative picture of the interplay between the 2SF and CSF phases in section 6.

Due to the 2BHCC, in the limit $\rho \to 2$, we may understand singly occupied sites (singlons) as moving on top of the fully occupied lattice $\cdots|2\rangle|2\rangle|2\rangle\cdots$. The singlons experience the effective dispersion:

$$\epsilon(k) = -2t\cos k + 2t'\cos 2k. \tag{5}$$

Hence, a sufficiently large density induces frustration for $t' > 0$, which is characterized as well by the presence of two degenerate minima in $\epsilon(k)$. We show below that this leads to the appearance of the CSF and the 2SF phases at large fillings.

4. Density-induced frustration

In this section we first consider the case of $t' > 0$, i.e. a model which is unfrustrated for low filling but becomes frustrated at large filling. Our DMRG results for the ground-state phase diagram of Model (1) with $U = 0$ are summarized in figure 2(b).

4.1. Gapless phases

In order to distinguish between gapped and gapless phases we evaluate the chemical potential μ obtained from the minimization of $E(L, N) - \mu N$, where $E(L, N)$ is the ground-state energy for N bosons in L sites [20]. The chemical potential as a function of the lattice filling for different values of t' is depicted in figure 3. Plateaus in this graph constitute a clear signature of the existence of gapped phases which will be discussed below. Furthermore the $\rho(\mu)$ curve for certain parameters exhibits a kink which signals a commensurate-

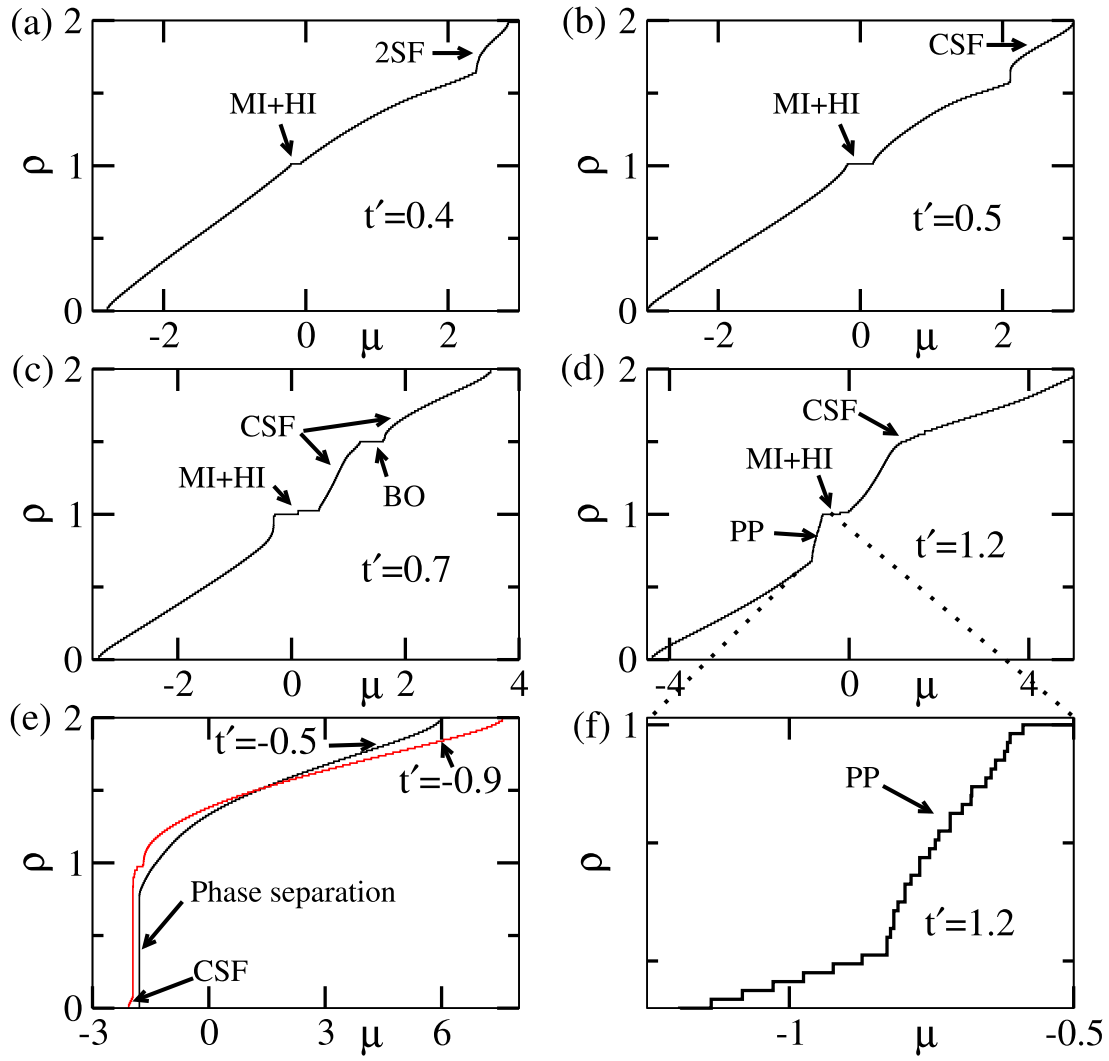

Figure 3. Curves $\rho(\mu)$ for $t' = 0.4$ (a), $t' = 0.5$ (b), $t' = 0.7$ (c), $t' = 1.2$ (d), and $t' = -0.5$ and -0.9 (e). The plateaus in (a), (b), (c) and (d) correspond to the gapped phases such as the MI+HI ($\rho = 1$) and the BO phase ($\rho = 1.5$). The macroscopic jump in (e) corresponds to the phase separation. (f) shows an enlarged view of the PP region in figure (d) which exhibits an unordered sequence of steps of one and two bosons.

incommensurate (C-IC) type transition [30] between a one-component SF phase and a two-component phase such as the 2SF or PP phase.

Whereas for low fillings the system is a simple SF phase, for $t' > 0.7$ and below $\rho = 1$ a different phase appears, the transition being identified by the kink as shown in figures 3(d) and (f). This phase is characterized by an increase of the filling for growing μ in an unordered sequence of steps of one and two bosons (see figure 3(f)). This feature is a signature of the so-called PP phase, a two-component superfluid phase of doublon- and holon-dimers characteristic of the one-dimensional anyon-Hubbard model [13]. In Model (1) the PP phase results from the quasi-anyonic character of the chains built up of even and odd sites, which become fully decoupled only in the limit $t' \gg t$. The PP phase survives in the region below unit filling for large values of t' as shown in the figure 2. As we will show below the PP-phase exhibits a multi-peak momentum distribution, since both holons and doublons may be treated as independent superfluids with different momenta.

Above unit filling, we observe C-IC transitions to a 2SF phase (again signaled by a kink in the $\rho(\mu)$-curve as depicted in figure 3(a)). This phase does not exhibit the PP-like feature discussed above. In the vicinity of the fully occupied lattice we may identify it with a 2SF phase of the frustrated zig-zag lattice from the dilute limit picture of sections 3 and 6.

With increasing t', the system enters a CSF phase, which is also stable for $\rho = 3/2$ when $t' > 1.0$ as discussed below. The CSF phase extends up to $\rho = 2$. We may clearly distinguish the CSF phase from the other phases by its non-vanishing chiral order parameter. The chiral order parameter κ as a function of ρ for three representative values of t' is plotted in figure 7. The current-current correlation function $\chi_i\chi_j$ is plotted in different regions of the phase diagram in the inset of figure 7. There is a sharp decay of the correlation function

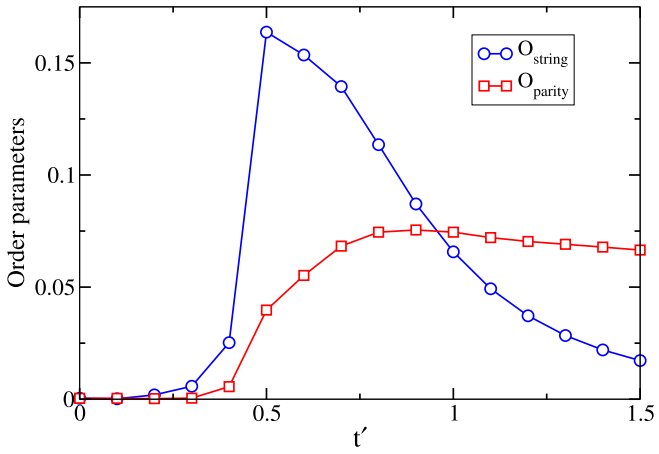

Figure 4. Extrapolated values of the string and the parity order parameters with respect to t' for $\rho = 1$. The simultaneous presence of both orders characterizes the MI+HI phase.

when the system is in the SF phase, whereas in the CSF phase the value of $\chi_i \chi_j$ shows a long-range correlation. The type of the 2SF–CSF transition which we expect to be of (weak) first order has to be clarified in further works.

For the case of very strong repulsive interactions where a mapping to a hardcore boson model is appropriate, we expect the same sequence of SF–2SF–CSF phases for the regime $1 < \rho < 1.5$ as discussed above for $\rho > 1.5$. Indeed also for $U = 0$ our numerical data is consistent with the presence of a small 2SF-phase separating the SF and the CSF phases.

4.2. Gapped phases

Since in Model (1) frustration emerges with growing filling we may expect the appearance of gapped phases for $U = 0$. As the hopping strength increases a gapped phase appears for $\rho = 1$ and $t' > 0.3$, whereas a second plateau is observed for $\rho = 3/2$ and $t' > 0.6$. These plateaus appear for a range of intermediate values of t' (see figures 3(a)–(d)) and then vanish for large t'. The extrapolated values of the chemical potentials corresponding to these plateaus are plotted in figure 2 (lobes bounded by black curves).

As mentioned above, a fully frustrated zig-zag lattice with 2BHCC exhibits a gapped HI phase for $U = 0$ at unit filling between the gapless SF and CSF phases. For larger values of $U > 0$ a Gaussian-type phase transition to a MI phase is induced [23]. Both the HI and MI phases exhibit different types of non-vanishing hidden orders. The MI phase is characterized by a finite parity-order parameter

$$O_{\text{parity}} = \lim_{|i-j|\to\infty} \langle (-1)^{\sum_{i<l<j} \delta n_l} \rangle, \tag{6}$$

with $\delta n_j = 1 - n_j$, which has been recently measured experimentally using single-site resolution [21]. Contrary to that the HI phase, which can be understood as a kind of a density wave (anitferromegnetic) ordered phase of doublons and holons diluted by single particles, exhibits a non-zero string-order parameter

$$O_{\text{string}} = \lim_{|i-j|\to\infty} \langle \delta n_i (-1)^{\sum_{i<l<j} \delta n_l} \delta n_j \rangle. \tag{7}$$

In a typical MI phase as studied in [23], one observes $O_{\text{parity}} \neq 0$ and $O_{\text{string}} = 0$ while for the HI phase, $O_{\text{parity}} = 0$ and $O_{\text{string}} \neq 0$. For the case of a broken space-inversion symmetry such as in Model (1), however, a smooth crossover between the HI and MI phases is observed [31]. Due to the direction-dependent tunneling a MI phase may exhibit a finite string order $O_{\text{string}} > 0$ because of the formation of quasi bound holon doublon pairs in one preferred direction as studied in [14, 32]. The gapped phase at $\rho = 1$ is a MI phase resulting from the density-induced frustration. In addition, and contrary to the usual MI, the gapped phase at $\rho = 1$ presents a non-zero string-order parameter. Figure 4 shows that both order parameters become finite around $t' \simeq 0.3$ where the gap opens. We hence denote this phase as the MI+HI phase in the phase diagram of figure 2.

In contrast, the gapped region at $\rho = 3/2$ is a BO phase that results solely from the density-induced geometric frustration. Due to the 2BHCC, doublons (i.e. doubly occupied sites) on top of the MI phase with all the sites occupied by one particle may be considered as hard-core bosons. The full state ($\rho = 2$) may be hence understood as an insulator with unit filling occupation ($\rho_D = 1$) of these hard-core bosons. The appearance of the BO phase can be hence understood from what is known for hard-core bosons in zig-zag lattices [24–26]. At density $\rho = 3/2$ ($\rho_D = 1/2$) the doublons minimize the energy by arranging themselves along the rungs of the

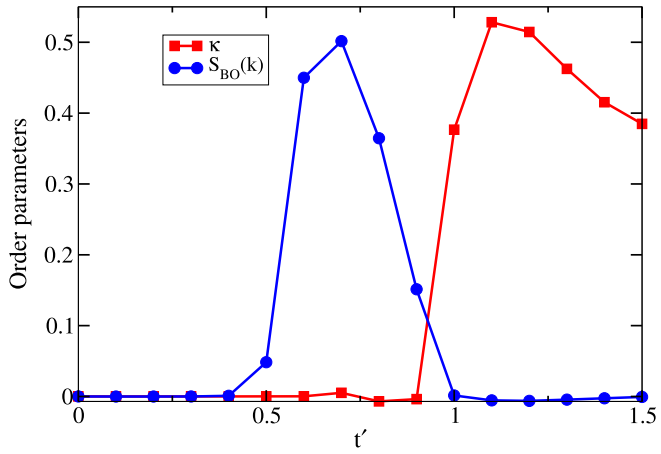

Figure 5. Extrapolated values of the bond-order structure factor $S_{\rm BO}(k=\pi)$ and the chiral order parameter κ, in the SF–BO–CSF region.

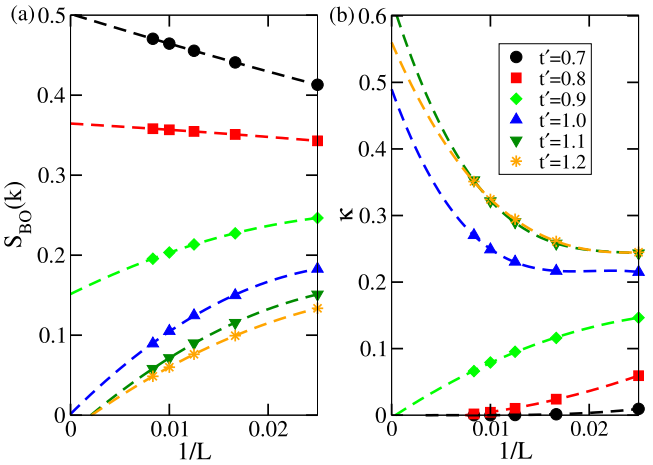

Figure 6. Finite size extrapolation of $S_{\rm BO}(k=\pi)$ (a) and κ (b) across the BO–CSF boundary.

ladder in a periodic pattern, which results in bond order. The existence of bond ordering is confirmed by a finite peak in the BO structure factor

$$S_{\rm BO}(k) = \frac{1}{L^2}\sum_{i,j} e^{ik(i-j)}\langle B_i B_j\rangle, \tag{8}$$

where $B_i = a_i^\dagger a_{i+1} + a_{i+1}^\dagger a_i$. By performing a finite size extrapolation of $S_{\rm BO}(k=\pi)$ using a polynomial of lowest order with system sizes of $L = 40, 60, 80, 100, 120$ we establish the existence of a BO phase for $0.4 < t' < 1.0$ as shown in figure 5 (blue circles). Upon increasing t' the system enters into the CSF phase, similarly as for the case of hardcore bosons [26]. The transition to the CSF phase at $\rho = 1.5$ is obtained by plotting the chiral order parameter. In figure 5 (red squares) we plot the extrapolated values of κ using system sizes of $L = 40, 60, 80, 100, 120$ which shows a transition to the CSF phase at $t' \sim 1.0$. The finite size extrapolation of $S_{\rm BO}(\pi)$ and κ is shown in figure 6. It can be clearly seen that $S_{\rm BO}(k)$ slowly goes to zero as t' increases and at the same time the value of κ becomes finite at $t' \simeq 1.0$.

5. Frustration decreasing with the density

For $t' < 0$ the system is frustrated as $\rho \to 0$, and for growing density the frustration is destroyed. One could hence naively expect an approximate inversion of the graph obtained for $t' > 0$. The situation is however rather different. For all $t' < 0$ we observe a large density jump for a fixed chemical potential (see figure 3(e) and the green squares in figure 2(a)). For $|t'| < 0.8$ the density jump starts from the vacuum, $\rho = 0$, whereas for $|t'| > 0.8$ there exists a finite CSF region at low densities. At $\rho = 1$ and $|t'| > 0.6$ we observe the MI+HI phase.

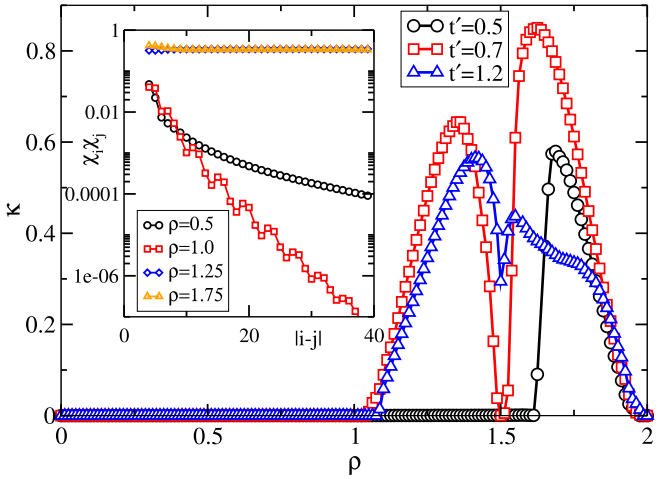

Figure 7. Chiral order parameter κ with respect to ρ for different t' at the transition to the CSF phase (see text). For $t' = 0.5$ (black circles) κ goes from zero to a finite value marking the SF to CSF phase transition. For $t' = 0.7$ (red squares), the region of finite κ is split into two parts by a region of $\kappa = 0$, marking the CSF–BO–CSF transitions (see figure 2(b)). For $t' = 1.2$ (blue triangles) the intermediate BO region has disappeared. The inset shows the current-current correlation $\chi_i \chi_j$ for different fillings.

Further increase in the density results in the SF phase. The presence of the strong density jump prevents the appearance of a BO phase at $\rho = 0.5$, the 2SF phase and the PP phase.

The presence of the density jump may be understood from the following simple argument. Due to the 2BHCC, $a_j^\dagger e^{i\pi n} a_{j+2} = a_j^\dagger (1 - 2n) a_{j+2}$. Although, the correction of the hopping depends on the number operator, we may understand the main effects of this correction by approximating in a mean field way $t' e^{i\pi n} \simeq t'_{\rm eff}(\rho) = t'(1 - \gamma\rho)$, where $\gamma > 0$ is a proportionality constant. For $t' > 0$, the single particle dispersion presents a single energy minimum at $k = 0$, with density-dependent energy per particle $E_0(\rho) = -2 - 2t'_{\rm eff}(\rho) = E_0(0) + 2t'\gamma\rho$. Note that the vacuum boundary is given by the curve $\mu = E_0(0)$. Since the energy increases with ρ the vacuum boundary is stable, and we expect a continuous growing of ρ as a function of μ. For $t' < 0$ the situation radically changes, as it is possible to see from the simple model above for $|t'| < 1/4$. There is still a single minimum at $k = 0$, but now with energy $E_0(\rho) = -2 + 2|t'_{\rm eff}(\rho)| = E_0(0) - 2|t'|\gamma\rho$, i.e. the energy decreases with ρ. As a result, when $\mu = E_0(0)$, the density-dependent hopping pushes $E_0(\rho)$ even further below μ, and hence ρ experiences a large jump corresponding to a negative compressibility (only arrested by corrections to the simple toy model).

6. Effective interaction in the limit $\rho \to 0$ and $\rho \to 2$

In the limits $\rho \to 0$ and $\rho \to 2$ we may derive an description of the system properties by means of a two-particle scattering problem [29, 33]. A general two-particle state may be described by

$$|\Psi_K\rangle = \sum_x c_{x,x} (b_x^\dagger)^2 |0\rangle + \sum_{x,y>x} c_{x,y} b_x^\dagger b_y^\dagger |0\rangle. \tag{9}$$

Due to the conservation of total momentum $K = k_1 + k_2$ in the scattering process one can express the amplitudes as $c_{x,x+r} = C_r e^{iK\left(x+\frac{r}{2}\right)}$. The Schrödinger equation $H|\Psi\rangle = \Omega|\Psi\rangle$ for the two-particle problem leads to the following system of coupled equations for the amplitudes C_r:

$$(\Omega - 2U) C_0 = -2\sqrt{2}\left(t \cos\left(\frac{K}{2}\right) C_1 - it' \sin(K) C_2\right), \tag{10}$$

$$\Omega C_1 = -2t \cos\left(\frac{K}{2}\right)(\sqrt{2} C_0 + s C_2) - 2t' s \cos K (C_3 + C_1), \tag{11}$$

$$\Omega C_2 = -2t \cos\left(\frac{K}{2}\right)(C_1 + C_3) - 2t'(\sqrt{2} i \sin(K) C_0 + s \cos(K) C_4), \tag{12}$$

$$\Omega C_r = -2ts \cos\left(\frac{K}{2}\right)(C_{r-1} + C_{r+1}) - 2t' s \cos(K)(C_{r-2} + C_{r+2}),\ r \geqslant 3. \tag{13}$$

For $\rho \to 0$ (2) we set $s = 1$ (2). The density-dependent term in Model (1) just enters through the sine function in the first and third equation (for the usual Bose–Hubbard model it would be a cosine). In the thermodynamic

limit the energy is given by $\Omega = \epsilon(k_1) + \epsilon(k_2) = -4\left(J\cos(k)\cos\left(\frac{K}{2}\right) + J'\cos(2k)\cos(K)\right)$ with the half relative momentum $k = (k_1 - k_2)/2$. For the scattering of two particles in the vicinity of the minimum at $Q = 0$ with momentum $k_1 = Q + k$ and $k_1 = Q - k$, i.e. total momentum $K = Q$, one may solve the system of equations with an Ansatz

$$C_r = \cos(kr + \delta) + \nu e^{-\kappa_0 r}. \tag{14}$$

The coefficients C_0, δ and ν are determined by equations (9)–(11), hence, are affected by the density-dependent hopping. The scattering lengths may be extracted from the scattering phase shift δ, $a = \lim_{k\to 0}\cot(\delta)/k$. One can relate the 1D scattering length to the amplitude of the contact interaction potential of the two-component Bose gas of mass m as $g = -2/ma$. For $|g|m \ll 1$ we may employ a continuum Lieb–Liniger model [29]. In this limit, for $g < 0$, the bosons form an attractively interacting model, characterized by the presence of bound states or a collapsing wave function.

For $|t'| \ll 1$, and after some algebra, we obtain:

$$g_{\rho\to 0} = \frac{U + 2t'(2 + 2t' + U)}{(1 + t'(2 + 2t' + U)} \simeq U + (4 - U^2)t', \tag{15}$$

$$g_{\rho\to 2} = \frac{2(3 + U + t'(11 + 8t' + 2U))}{1 + 2t'(4 + 4t' + U)} \simeq 6 + 2U - 2t'(13 + 2U(6 + U)) \tag{16}$$

For $U = 0$, $g_{\rho\to 0} = 4t'$, and hence for $t' < 0$ an effective attraction is realized, providing an alternative intuitive picture of the instability observed in the $\rho(\mu)$ curve. In contrast, $g_{\rho\to 2} = 6(1 - 6t')$ remains positive for any small t', leading to an effective repulsive interaction even for $U \to 0$ due to the density-dependent frustration.

For the case of two degenerate minima these arguments may be generalized. One may consider both dispersion minima as two distinct species of particles. The low-energy properties are determined by both the scattering from particles of the same minimum and scattering of particles from different dispersion minima, which give rise to effective intra- and inter-species interactions. For the case of a dominant intra-species interaction both minima are occupied and a 2SF-phase is stabilized. A dominant inter-species coupling will lead to a CSF phase in the dilute limit. For a detailed calculation we refer to [29]. For this case we determine the 2SF–CSF transition for $t' \approx 0.97t$ for the case $\rho \to 2$ which only coincides qualitatively with our DMRG calculation (as shown in figure 2 we could determine the boundary around $t' \approx 0.4t$) showing that at large t'/t the CSF phase is favored. This discrepancy has been reported already in [26, 29, 34] and is possibly due to the difficulty in determining the CSF–2SF boundary accurately at low or large fillings numerically because of vanishing chiral order parameter.

7. Experimental signature

In order to obtain the signatures of the quantum phases we compute the momentum distribution function

$$n(k) = \frac{1}{L}\sum_{i,j} e^{ik(i-j)}\langle a_i^\dagger a_j\rangle. \tag{17}$$

where $\langle a_i^\dagger a_j\rangle$ is the single particle correlation function. We plot $n(k)$ as a function of ρ along two representative cuts through the phase diagram, $t' = 0.7$ and 1.5, as shown in figure 8.

For $t' = 0.7$, as the system goes from SF–MI–CSF–BO–CSF as a function of ρ, we observe for growing ρ regions of different momentum distributions: a single peak of $n(k)$ at $k = 0$ (SF), no peak (HI+MI at $\rho = 1$), two peaks at $\pm k$ (CSF), no peak (BO at $\rho = 3/2$), and again two peaks at $\pm k$ (CSF). Note that in the CSF phase a single experimental realization will typically just observe one peak at $+k$ or at $-k$ corresponding to one of the two degenerate groundstates as discussed in [2]. For $t' = 1.5$, we observe a markedly different dependence for growing ρ: a region with a single momentum peak (SF), then a region with multiple peaks (PP), no peak (MI +HI at $\rho = 1$), and two peaks at $\pm k$ (CSF). The momentum distribution, which may be extracted from standard time-of-flight measurements, constitutes hence an excellent experimental observable for the observation and characterization of the different phases.

8. Conclusions

Laser-assisted hopping may result in density-dependent magnetism, and more generally in density-dependent frustration. In this paper we have illustrated the consequences that density-induced frustration (together with 2BHCC) may have on the properties of a bosonic gas, for the particular case of bosons in a zig-zag lattice in which the sign of the next-to-nearest hopping (and hence the geometric frustration) depends on the local occupation. We have shown that, even in the absence of two-body interactions ($U = 0$) the density-dependent frustration

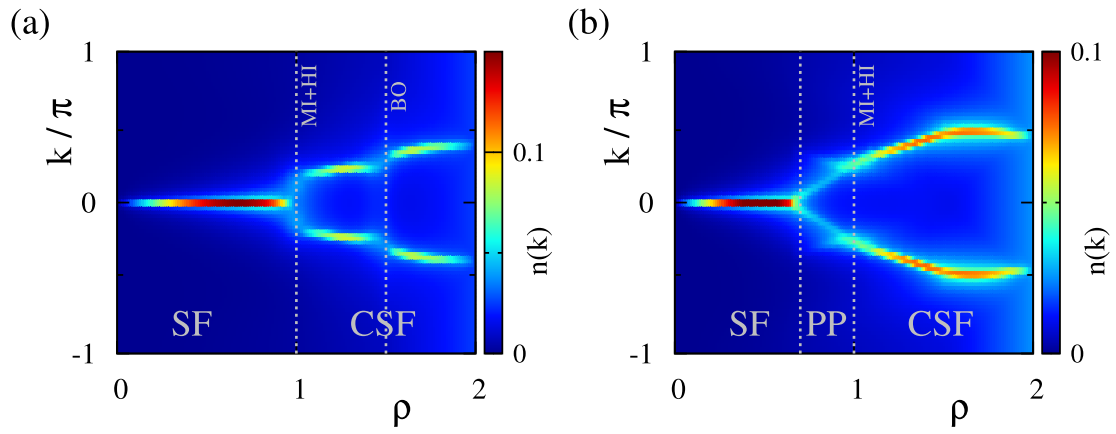

Figure 8. Momentum distribution function $n(k)$ for $t' = 0.7$ (a) and $t' = 1.5$ (b). Note the different form of $n(k)$ for the different phases of the system.

leads to a wealth of gapped (MI+HI, BO) and gapless (SF, 2SF, CSF, PP) phases, since for $t' > 0$ the system basically interpolates for growing filling from a non-frustrated non-interacting system to a fully frustrated system with an effective two-body repulsion induced by the density-dependent hopping. In contrast, for $t' < 0$, frustration decreases with density, but the frustrated low density regime is unreachable due to the vacuum destabilization resulting from the effective inter-particle attraction induced for $t' < 0$ by the density-dependent hopping. Finally, we have shown that the discussed phases may be experimentally revealed in time-of-flight measurements due to their different signatures in the momentum distribution.

Acknowledgments

We acknowledge support from the Center for Quantum Engineering and Space Time Research and the Deutsche Forschungsgemeinschaft(Research Training Group 1729). Simulations were performed on the cluster system of the Leibniz Universität Hannover.

References

[1] Lewenstein M, Sanpera A and Ahufinger V 2012 *Ultracold Atoms in Optical Lattices: Simulating Quantum Many-Body Systems* (Oxford: Oxford University Press)
[2] Struck J *et al* 2012 *Phys. Rev. Lett.* **108** 225304
[3] Jo G B *et al* 2012 *Phys. Rev. Lett.* **108** 045305
[4] Wirth G, Ölschläger M and Hemmerich A 2012 *Nat. Phys.* **7** 147
[5] Tarruell L *et al* 2012 *Nature* **483** 302
[6] Struck J *et al* 2011 *Science* **333** 996
[7] Aidelsburger M *et al* 2013 *Phys. Rev. Lett.* **111** 185301
[8] Miyake H *et al* 2013 *Phys. Rev. Lett.* **111** 185302
[9] Atala M *et al* 2014 *Nat. Phys.* **10** 588
[10] Mancini M *et al* 2015 *Science* **349** 1510
[11] Stuhl B K *et al* 2015 *Science* **349** 1514
[12] Keilmann T *et al* 2011 *Nat. Commun.* **2** 361
[13] Greschner S and Santos L 2015 *Phys. Rev. Lett.* **115** 053002
[14] Greschner S *et al* 2015 *Phys. Rev.* B **92** 115120
[15] Bermudez A and Porras D 2015 *New J. Phys.* **17** 103021
[16] Kolezhuk A K 2002 *Prog. Theor. Phys. Suppl.* **145** 29
Kolezhuk A K 2000 *Phys. Rev.* B **62** R6057
[17] Vekua T, Honecker A, Mikeska H-J and Heidrich-Meisner F 2007 *Phys. Rev.* B **76** 174420
[18] Hikihara T, Kaburagi M, Kawamura H and Tonegawa T 2000 *J. Phys. Soc. Japan* **69** 259
[19] Hikihara T 2002 *J. Phys. Soc. Japan* **71** 319
[20] Hikihara T, Kecke L, Momoi T and Furusaki A 2008 *Phys. Rev.* B **78** 144404
[21] Sherson J F *et al* 2010 *Nature* **467** 68
[22] Hikihara T, Momoi T, Furusaki A and Kawamura H 2010 *Phys. Rev.* B **81** 224433
[23] Greschner S, Santos L and Vekua T 2013 *Phys. Rev.* A **87** 033609
[24] Mishra T, Pai R V, Mukerjee S and Paramekanti A 2013 *Phys. Rev.* B **87** 174504
[25] Mishra T, Pai R V and Mukerjee S 2014 *Phys. Rev.* A **89** 013615
[26] Mishra T, Greschner S and Santos L 2015 *Phys. Rev.* A **91** 043614
[27] White S R 1992 *Phys. Rev. Lett.* **69** 2863
[28] Schollwöck U 2005 *Rev. Mod. Phys.* **77** 259

[29] Kolezhuk A K, Heidrich-Meisner F, Greschner S and Vekua T 2012 *Phys. Rev.* B **85** 064420
[30] Piraud M *et al* 2015 *Phys. Rev.* B **91** 140406
[31] Pollmann F *et al* 2010 *Phys. Rev.* B **81** 064439
[32] Greschner S, Santos L and Poletti D 2015 *Phys. Rev. Lett.* **113** 183002
[33] Azimi M *et al* 2014 *Phys. Rev.* B **89** 024424
[34] Mishra T, Greschner S and Santos L 2015 *Phys. Rev.* B **92** 195149